UDC 669.184

Solid-liquid mass transfer in a Peirce-Smith converter: A physical modelling study

Deside Kudzai Chibwe[1], Guven Akdogan[1], Jacques Eksteen[2]

[1] *Process Engineering Department, University of Stellenbosch, P Bag X1, Stellenbosch, South Africa, 7602*
[2] *Lonmin Western Platinum Limited, Process Division, P Bag X508, Marikana, South Africa, 0284*

Pyro-metallurgical processes are multiphase in nature involving gas-liquid-solid interactions. In the Peirce-Smith converter operation, the additions of cold solids in liquid matte in the form of fluxing agents (silica sands) for slag liquidity, process scrap and reverts for temperature control is a common practice. It is reasonable to postulate that with such practice, solid-liquid mass transfer step may play an important role in the performance and attainment of liquid bath homogeneity of the process. In this work, solid additions were simulated with sintered benzoic acid compacts spatially positioned in a 1:5 water model of a Peirce-Smith converter. Water and kerosene were used to simulate matte and slag respectively. Solid-liquid mass transfer was characterized by experimentally determined mass transfer coefficient, K (ms^{-1}) values of benzoic acid sintered compacts and calculated dimensionless turbulence characteristic, T_c values. The mass transfer coefficients and dimensionless turbulence characteristic values were highest at the bath surface and near plume region. The values decreased in identified dead zones in the regions close to the circular side walls of the model. The results revealed that the mass transfer coefficients and turbulence characteristics were different with respect to different submergence levels of the compacts. These findings lead to the conclusion that the fluid flow was stratified within the vessel.

Keywords: PHYSICAL MODELLING, PEIRCE-SMITH CONVERTER, MASS TRANSFER

Introduction

In copper and PGMs smelters, liquid matte from primary furnaces is chemically associated with iron (Fe) and sulphur (S) as chemical impurities attached to Cu and Cu-Ni respectively. Removal of the impurities is carried out in a Peirce-Smith converter (PSC) through an oxidation process. The process reactions are highly exothermic in nature and high temperatures could result depending on the grade of charged matte. It has become an inherent process characteristic to add cold flux and scrap, process reverts and ladle skulls in order to control thermodynamics of the process. Solid-liquid mass transfer step may play an important role in the performance and attainment of thermal and chemical bath homogeneity.

The mechanism and behavior of dissolution of the cold additions and active sites within the converter is not well understood. Rates of dissolution can be assumed to affect the thermal state of the converter and hence to be a factor that affects the turnaround time of the converter processing. Therefore, establishing a stable functional state of the converter and fully developed categorization of flow fields is necessary for effective process control.

However, there are no literature sources that have been found addressing this critical subject of solid-liquid interactions in PSC. The only source close to the subject is the study conducted by [1], who studied gas-phase mass transfer in a PSC using physical model. Their work revealed pertinent information relating to oxygen utilization efficiency in the converter. They found that gas at high injection rates was under-utilised.

Literature pertaining to solid-liquid mass transfer in ladle metallurgy is fairly comprehensive. Pioneering work to investigate solid-liquid mass transfer phenomena in turbulent circulatory flows was conducted by [13]. In this work, dissolution patterns of immersed graphite rods in Ar-stirred melts with the experimental

measurement results have been interpreted with two-equation ($k-\varepsilon$) model. Mass transfer data was expressed in the form of dimensionless Sherwood number, Sh which represents the ratio of convective to diffusive mass transport relating the physical properties of the system to the mass transfer coefficient. Simplified expression of Sherwood number is written as

$$Sh = \frac{Kd}{D_o} \qquad \text{(Eq. 1)}$$

In this **Eqn 1**, K (ms^{-1}) is mass transfer coefficient, d (m) is a characteristic dimension and D_o (m^2s^{-1}) is diffusivity. In the work done by [13], the Sherwood number functional relationship was expressed in the form of power series as a function of flow local Reynolds number, $\mathrm{Re}_{loc,r}$, turbulent Reynolds number, Re_t and Schmidt number, Sc. The Schmidt number explicitly characterise fluid flow in terms of momentum (viscosity) and mass diffusivity in a mathematical expression as

$$Sc = \frac{\mu}{\rho D_o} = \frac{v}{D_o} \qquad \text{(Eq. 2)}$$

In **Eqn 2**, μ (Pas) is dynamic viscosity, ρ (kgm^{-3}) is fluid density and v (m^2s^{-1}) is kinematic viscosity. The correlation proposed by [13] was derived for unidirectional flow conditions with the assumption that flow is normally directed to the surface of the solid objects. Inherently, metallurgical process systems are multi-dimensional in nature and this shortfall preluded application of the proposed correlation. [9] manipulated the proposed correlation of [13] by commissioning a more plausible definition of Reynolds number and turbulence characteristic, T_c on the basis of fluid resultant velocity, v_r (ms^{-1}), local fluctuating velocity, v' (ms^{-1})and local mean velocity, $\bar{v}$ (ms^{-1}) components. Such considerations reflected the influences of multi-dimensional flow system on the mass transfer phenomena. The proposed correlation is presented by

$$Sh = 0.73\left(\mathrm{Re}_{loc,r}\right)^{0.25}\left(\mathrm{Re}_t\right)^{0.32}\left(Sc\right)^{0.33} \qquad \text{(Eq. 3)}$$

A comprehensive assessment of the adequacy and appropriateness of various Sherwood number based correlations for estimating mass transfer rates was conducted [11]. This work conclusively recommended that the correlation given by equation (3) is likely to provide reasonable estimates of solid-liquid mass transfer rates in gas bubble systems due to the conformance between measured and predicted distribution of flow parameters and various dimensionless groups notably local Reynolds number, $\left(\mathrm{Re}_{loc,r}\right)$, turbulent Reynolds number, $\left(\mathrm{Re}_t\right)$ and Schmidt number, $\left(Sc\right)$.

In the current study, we aim to characterize the spatial behavior of the PSC regions as a function of mass transfer activities. This is carried out through calculation of the localized turbulence characteristic, T_c and mass transfer coefficient, K values of benzoic acid compacts placed in different converter locations. The dependence of these two mass transfer parameters on operating system variables such as air flow rate, Q and the presence of second phase (slag) are investigated. Since hydrodynamic studies are only concerned with geometric and dynamic similarity effects, only these two similarity conditions were observed in this work [8]. A 1:5 water bath physical model of a generic industrial (prototype) PSC used in copper smelters was used to carry out the investigations. The modified Froude number, N^*_{Fr} which resembles fluid flow dominated by inertial and gravitational forces as in the current study was used for dynamic similarity. The molten liquid phases in the real PSC namely matte and slag were simulated in the model with water and kerosene respectively.

Methodology

The experimental setup used in the current study has been discussed comprehensively [3, 4]. As such, only the more important aspects will be given in this text. As mentioned earlier, the modified Froude number, N^*_{Fr} was considered as the similarity criterion to correlate the air flow rate, Q between the model and the prototype system as applied in earlier studies [7, 10].

$$N^*_{Fr} = \frac{v_t^2 \rho_g}{g\left(\rho - \rho_g\right) d_o} \qquad \text{(Eq. 4)}$$

In the above equation, v_t (ms^{-1}) is tuyere air velocity, ρ_g (kgm^{-3}) is air density, g (ms^{-2}) is gravitational constant, d_o (m) is tuyere diameter.

Through application of (4), prototype nominal air flow rate has scaled down to $0.01125 Nm^3s^{-1}$ for

the water based model. This air flow rate will be referred to as Q_m^* in this work.

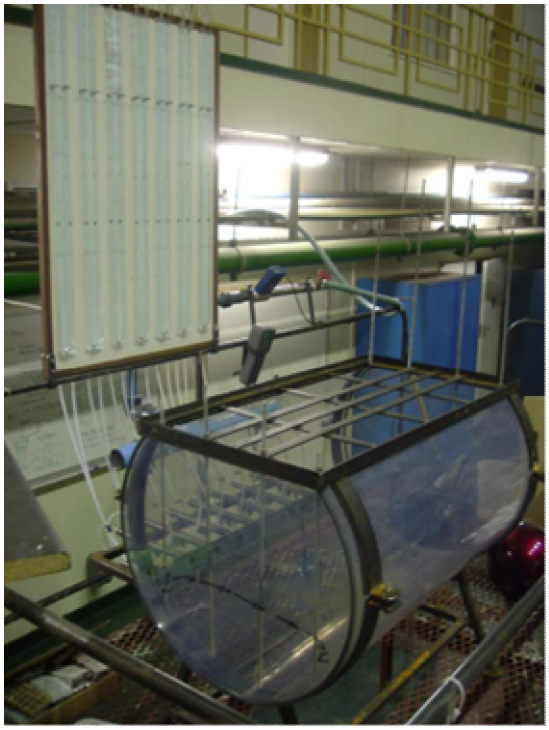

Figure 1. Pictorial assembly of the developed water bath model of a Peirce-Smith converter

In the experiments conducted in this work, we considered three air flow rates given by 0.01125 ± 0.0025 Nm^3s^{-1}. Also, two simulated slag thickness, SS_t of 54mm and 108mm were used in the experiments, representing 20% and 40% of simulated matte height respectively. These two simulated slag volumes will be referred to as low simulated slag, SS_{Low} and high simulated slag, SS_{High} volumes respectively in this text. The physical model derived from the similarity criterion, used in the current investigation is given in **Figure 1**.

Commercial benzoic acid flake was melted and casted into cylindrical benzoic acid compacts through a sintering cycle in a muffle furnace as given in **Figure 2**. The samples produced were 0.081m long; 0.038m diameter. To promote radial dissolution and minimize the end effects, the samples were enclosed between two thin mild steel washers on both ends.

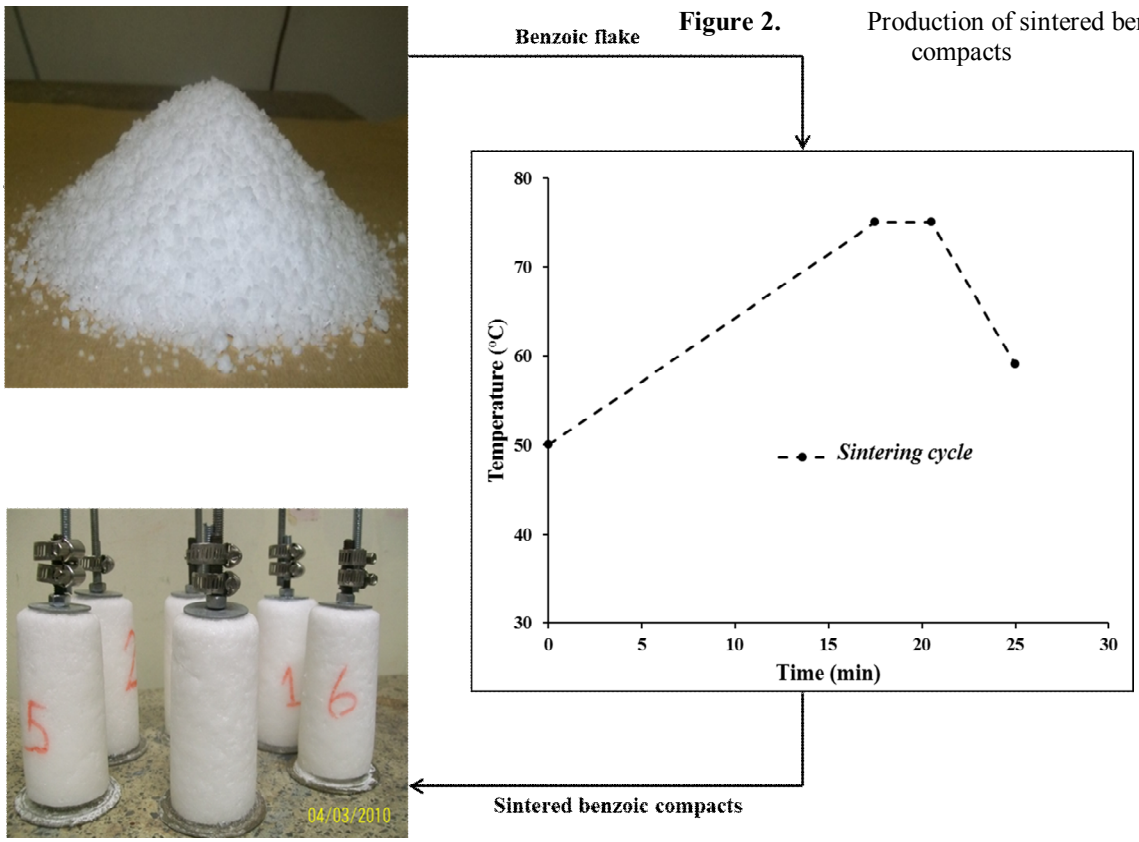

Figure 2. Production of sintered benzoic acid compacts

The benzoic acid compacts were mounted to a steel grid fastened with threaded rod as shown in **Figure 2** (bottom-left picture). A total of 8 samples were spatially located in the converter model at predetermined depth for every experimental run as shown in **Figure 3**. The sample labelling convention used here shows sample number and submergence referenced from the converter bottom. Due to shallow simulated matte depth relative to the sample lengths, L only two sample depths were considered in these experiments. H_{50} and H_{90} represents sample depth which are 50mm and 90mm from converter bottom respectively.

The samples were introduced and immersed into the water bath after the required air volumetric flow rate has reached a steady state value within +/-1% of the required value and the simulated slag thickness has been added. The samples were simultaneously subjected to 4 cycles of 900 seconds treatment, for which intermittently, they were removed, thoroughly dried and weighed. A weight loss measurement technique was employed to convert the weight loss into equivalent radii, R (m) so as to calculate mass transfer coefficients, K based on the film based mass transfer model equation given by (5) as described in earlier research [15].

$$-\frac{dM}{dt} = KA\left(C_s^* - C_b\right) \qquad \text{(Eq. 5)}$$

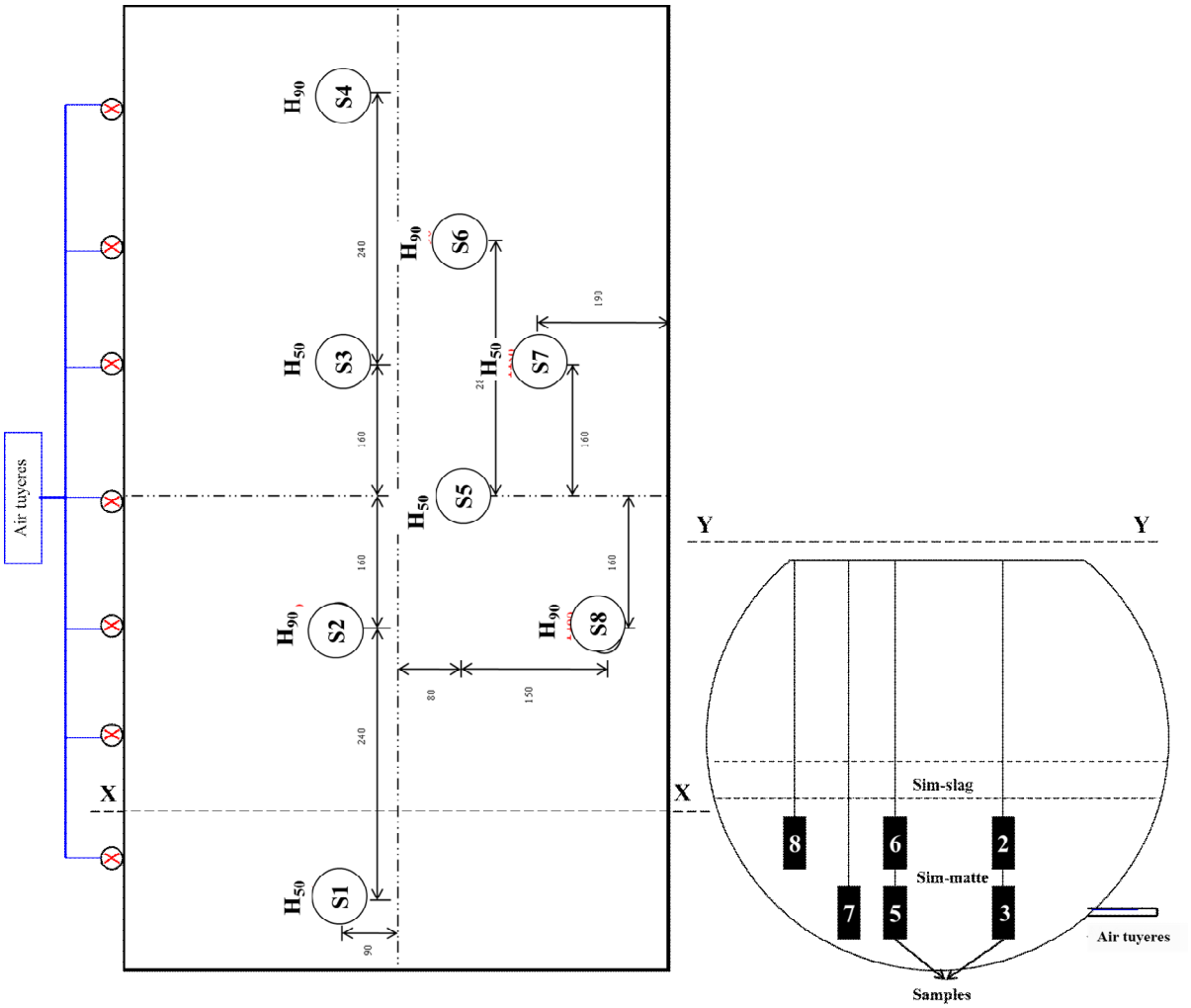

Figure 3. Schematic top and side view of the samples spatial locations in the converter model

In the equation above, A (m^2) is sample exposed surface area, M (g) is sample mass, t (s) is time, C_s^* (gl^{-1}) is solute saturation concentration, C_b (gl^{-1}) is instantaneous solute concentration. In formulation of equation (5), two major assumptions made were that the concentration of the liquid at the sample surface is equal to the saturation concentration of sample in solution and the effective driving force for interfacial mass transfer across the effective liquid film which surrounds the sample is the difference between the saturated solute concentration at the sample surface and the concentration in the bulk liquid as indicated by earlier studies [1, 5, 6].

Furthermore, considering $M = \rho_s \pi R^2 L$ and $A = 2\pi RL$ together with the assumption that C_b is relatively small and negligible where, ρ_s (kgm^{-3}) is sample density, the mass transfer coefficient, K in equation (5), can be presented as

$$K = -\left(\frac{dR}{dt}\right)\frac{\rho_s}{C_s^*} \qquad \text{(Eq. 6)}$$

Through rearranging equation (3), we obtain a turbulence characteristic equation which contains dimensionless groups namely kinematic viscosity, diffusivity and geometrical effects of the model as given in equation (7) below.

$$T_c = \left(\mathrm{Re}_{loc,r}\right)^{0.25}\left(\mathrm{Re}_t\right)^{0.32} = \frac{Sh}{0.73(Sc)^{0.33}} \qquad \text{(Eq. 7)}$$

This equation is used to characterize the turbulence effect as it effectively resolves fluctuating components of integral flow quantities of velocity and turbulence as applicable to the current study. There was no data available in literature for kerosene-water emulsions thermophysical properties. However it is known that emulsion viscosities are higher than the viscosities of individual components and as such in this work we assumed the emulsion to have average properties equivalent to water properties. Thermophysical properties and relevant data employed in the present investigation are given in **Table 1**.

Table 1. Thermophysical properties and data used in the current work

Property	Value
Molecular weight of benzoic acid (g)	122.12
Density of benzoic acid (kgm^{-3})	1260
Solubility of benzoic acid in kerosene-water emulsion (gl^{-1})	4.074
Kinematic viscosity of kerosene-water emulsion (m^2s^{-1})	1002×10^{-9}
Diffusivity of benzoic acid in kerosene-water emulsion (m^2s^{-1})	2.0×10^{-9}

Results and Discussion

Typical sample radii decay curve by the dissolution of benzoic acid compacts in simulated slag-matte system is shown in **Figure 4**. From these results, Sherwood numbers, solid-liquid mass transfer coefficients and turbulence characteristics values were calculated using equations (1), (5) and (6).

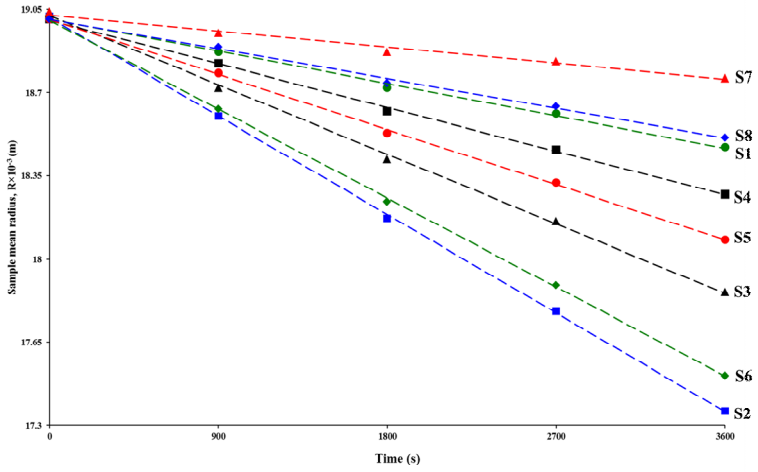

Figure 4. Sample radius decay with time at $0.01125 Nm^3s^{-1}$ with 54mm simulated slag thickness

Dissolution characteristics with respect to location

Considering **Figure 4**, which shows sample radii decay curve by the dissolution of benzoic acid compacts, we observed some preferential dissolution behavior. As expected, the dissolution varied with respect to all air flow rates and simulated slag volumes considered in this study. Sample locations that have shown dissolution behavior of interest are S2 and S3 (Refer to **Figure 2** for the locations). S2 which lies in the same location as S3 with respect to tuyere position but close to the simulated slag-matte interface exhibited the higher dissolution rate compared to S3. On the other hand, Sample S6 which is also near the simulated slag-matte interface exhibited second highest dissolution rate ahead of S5. These observations indicated that there exists a circulatory and stratified flow behavior which potentially have different velocity flow variable with respect to the depth of the samples in the simulated liquids. This observation is consistent with earlier study [14]. In their work, they measured experimentally and numerically liquid velocity distributions in a water model of a Peirce-Smith converter. Their study identified a circulatory flow field in the converter with higher velocities experienced near bath surface. In the current work, this phenomenon is further attested to by behavior of S7 and S8 with S8 experiencing high dissolution rates than S7. S1 and S4 also confirmed flow stratification, with high dissolution being experienced on S4 which is near slag-matte interface. It is also instructive to notice that both S1 and S4 had lower dissolution rates compared to S2, S3, S5 and S6. This observation serves to highlight that S1 and S4 are positioned in dead zones near the converter side walls in the model.

Dissolution characteristics with respect to flow variables

Two trends of dissolution behavior were observed in terms of K and T_c values as a function of simulated slag volumes and air flow rate. The trends were observed for SS_{Low} and SS_{High} as air flow rate increased from 0.00875Nm^{3}s^{-1} (22% < Q_m^*) to 0.01375Nm^{3}s^{-1} (22% > Q_m^*) irrespective of location in the converter as shown in **Figures 5** and **6.**

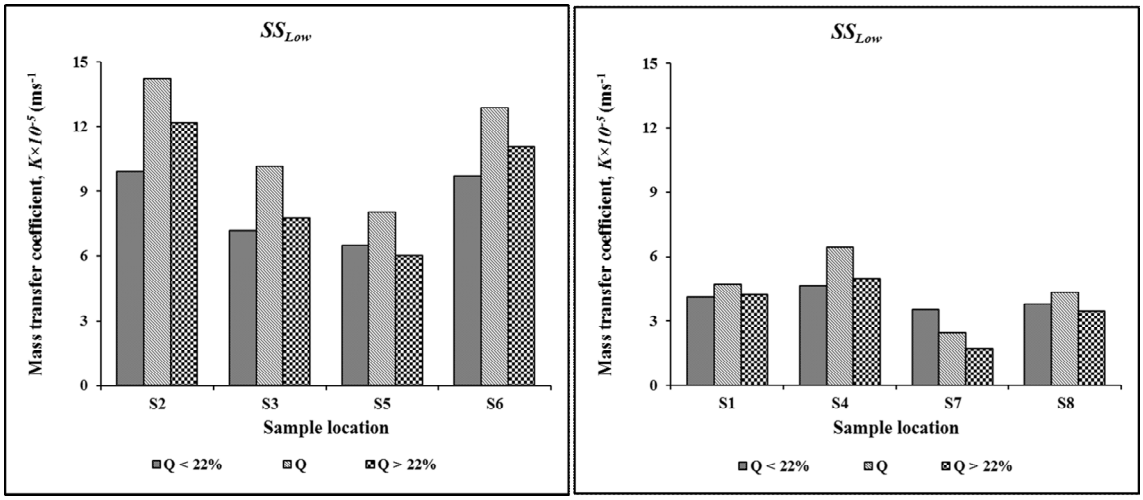

Figure 5. Variation of mass transfer coefficients with air flow rate, Q (=Q_m^*) at low simulated slag volume a) high and b) low dissolution sample locations

From **Figure 5**, it can be seen that the values of K increased as air flow is increased from 0.00875Nm^{3}s^{-1} to Q_m^*. This is possibly due to increased fragmented body forces between the sample and emulsion which increases the transport process as air flow rate increases. However, with further increase in air flow to 0.01375Nm^{3}s^{-1}, we observed a decrease in mass transfer values. Due to shallow submergence of the tuyeres, channelling phenomena becomes prevalent at high air flow rates [1]. Channelling will cause a breakdown on energy transfer to the system hence reduction in the transport process which resulted in the observed decrease in transport variable.

However with high simulated slag volumes, SS_{High}, we observed a decrease in K values as air flow is

increased from 0.00875 Nm^3s^{-1} to Q_m^* as shown in **Figure 6**. It is possible that at these high slag volumes, phase interactions and interphase friction is highly pronounced so much that fragmented body forces between the sample and emulsion are weakened thereby retarding the transport process. Noticeable increase in the mass transfer parameters were observed with an increase in air flow to 0.01375Nm^3s^{-1}.

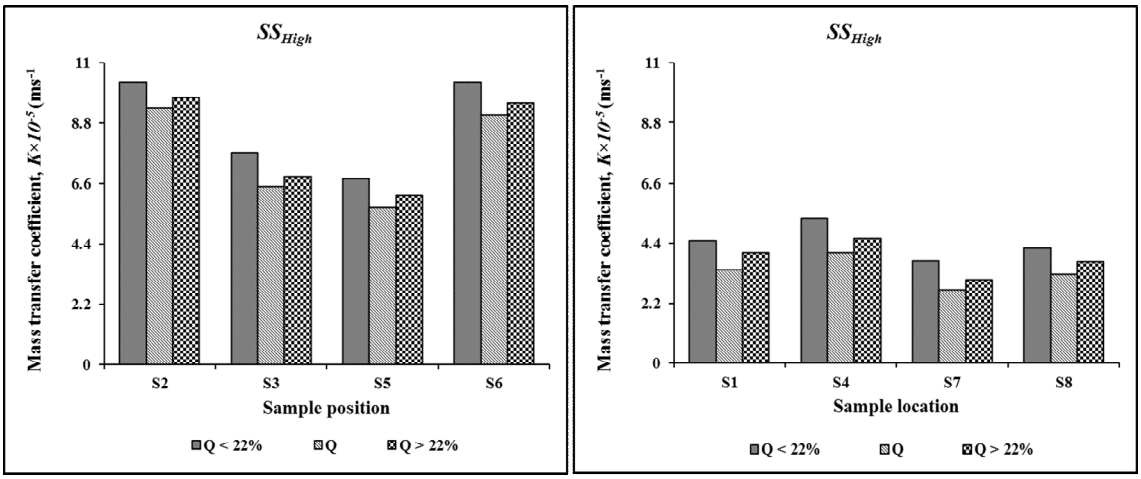

Figure 6. Variation of mass transfer coefficients with air flow rate, Q (=Q_m^*) at high simulated slag volume a) high and b) low dissolution sample locations

This increase could reasonably be as a result of increased energy input to the system, the situation being sustained by marginally deep submergence caused by high slag volume which allows for effective air-liquid momentum exchange. With the above facts in mind, it should be noted that the magnitude of mass transfer values achieved with SS_{High} and air flow rate 22% above Q_m^* is still short compared to the values achieved with SS_{Low} at Q_m^*. This scenario depicts under-utilisation of capacity in terms of energy at high simulated slag volumes.

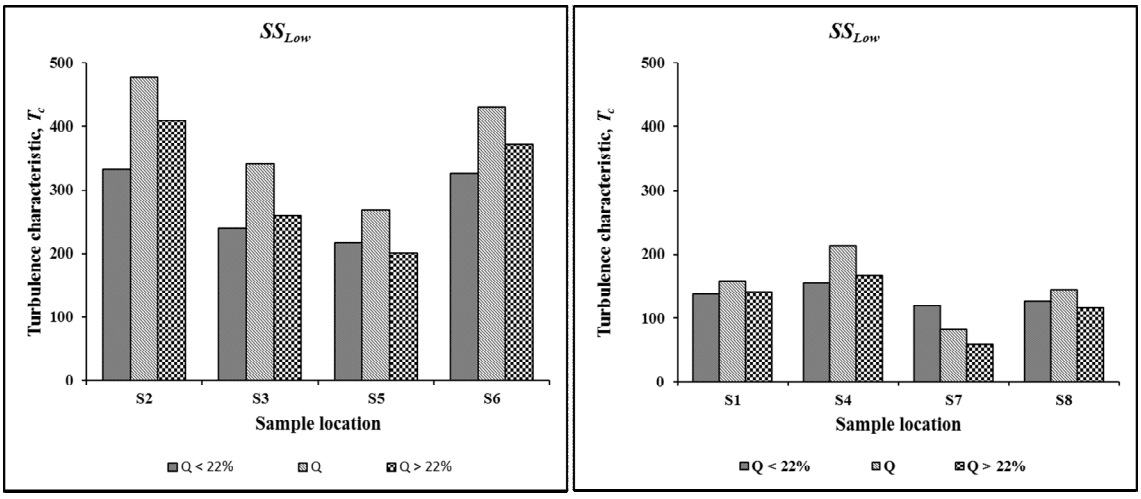

Figure 7. Variation of turbulence characteristic with air flow rate, Q (=Q_m^*) at low simulated slag volume a) high and b) low turbulence characteristic sample locations

Using equation 7, turbulence characteristic values were calculated in respect to sample locations in the model. **Figure 7** gives results obtained at low simulated slag volume. It was observed that the responds to flow variables for experimental mass transfer coefficient and calculated turbulence characteristic values was the same as shown by **Figures 5** and **7**. There is good agreement in

responds to change in air flow rate and simulated slag volumes as given in **Figure 8**.

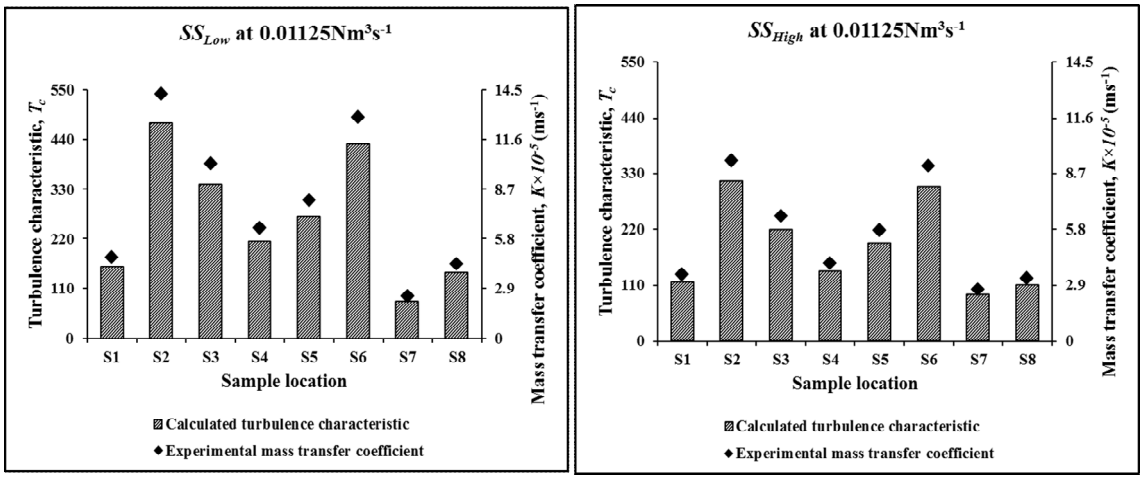

Figure 8. Comparison of experimental mass transfer coefficient and calculated turbulence characteristic values

The observed mass transfer behavioural responds to air flow rate and simulated slag volumes is a culmination of complex interaction of emulsification degree (entrainment), air-liquid momentum exchange interaction (retention) time and interphase friction concepts of slag into matte. However, in view of an earlier study [12], enhanced emulsification in slag-matte systems has been shown to better metallurgical reactions and operational improvement due to increased interfacial area for reactions. In the system under current study, emulsification/ entrainment of simulated slag droplets into simulated matte was observed as well. The degree of entrainment increased with air flow rate. From process reaction kinetics, we expect the converter to have high slag-matte reaction efficiency. It is instructive however to highlight the shortfall of under-utilization of energy at high air flow rates due to channelling effects caused by inherent shallow depth of tuyeres in Peirce-Smith converter operation as compared to bottom blown vessels.

Conclusions

A 1:5 water model of a Peirce-Smith converter has been developed to study solid-liquid mass transfer phenomena with an objective of spatial mapping the converter regions. Three air flow rates centralised at equivalency prototype nominal air flow rate and two simulated slag volumes were considered to represent the low and high slag volumes. Sintered benzoic acid compacts simulating solid additions in the converter were used. Based on the mass transfer measurements on the dissolution behaviour of the compacts and calculated turbulence characteristic values, the following conclusions can be drawn for solid-liquid mass transfer in a Peirce-Smith converter;

1) Flow pattern in Peirce-Smith converters is found to be stratified with high bath velocities experienced near bath surface regions. A recirculation loop is originated from the plume region to the bulk of the liquid matte.

2) It was revealed that both air flow rate and slag quantities affects dissolution behavior in slag-matte systems. High slag volumes are detrimental to the process efficiency as they results in potential pronounced interphase friction thereby reducing the transport process in the converters and it can be inferred that solid-liquid mass transfer rates can be effectively controlled by close monitoring of slag quantities and air flow rates.

3) There were dead zones observed close to the side walls of Peirce-Smith converter as observed by poor dissolution rates in those regions.

4) The results in this work have demonstrated that the calculated turbulence characteristic sufficiently estimates mass transfer in the model as the two parameters exhibited same responds to change in flow conditions.

References

1. Adjei, E. and Richards, G.G., 1991. Physical Modelling of Mass Transfer in a Peirce-Smith Converter. Copper 91(Cobre 91), IV, pp. 377-388.
2. Arters, D.C. and Fan, L.S., 1986. Solid-liquid mass transfer in a gas-liquid-solid fluidized bed. Chemical Engineering Science, 41(1), pp. 107-115.
3. Chibwe, D.K., Akdogan, G., Aldrich, C. and Eric, R.H., 2011a. CFD Modelling of Global Mixing Parameters in a Peirce-Smith Converter with Comparison to Physical Modelling. Chemical Product and Process Modeling, 6(1), pp. 22-52.
4. Chibwe, D.K., Akdogan, G., Aldrich, C. and Taskinen, P., 2011b. Characterisation of phase distribution in a Peirce-Smith converter using water model experiments and numerical simulation. Research Article edn. Mineral Processing and Extractive Metallurgy (Trans. Inst. Min Metall. C): Maney. DOI 10.1179/1743285511Y.0000000017
5. Jameson, G.J., 1964. Mass (or heat) transfer from an oscillating cylinder. Chemical Engineering Science, 19(10), pp. 793-800.
6. Kim, S.H. and Fruehan, R.J., 1987. Physical modeling of liquid/liquid mass transfer in gas stirred ladles. Metallurgical and Materials Transactions B, 18(2), pp. 381-390.
7. Koria, S.C. and Shamsi, M.R.R.I., 1990. Simulation of Mass Transfer from Metal to Slag in Gas Stirred Ladles. Ironmaking and Steelmaking, 17(6), pp. 401-409.
8. Mazumdar, D., 1990. Dynamic similarity considerations in gas-stirred ladle systems. Metallurgical and Materials Transactions B, 21(5), pp. 925-928.
9. Mazumdar, D., Kajani, S.K. and Ghosh, A., 1990. Mass transfer between solid and liquid in vessels agitated by bubble plume. Process Metallurgy steel research, 61(8), pp. 339-346.
10. Robertson, D.G.C., Conochie, D.S. and Castillejos, A.H., 1980. Model Studies on Gas-and-Solid Injection and Related Phenomena in Liquid Metal Baths. Scaninject II, , pp. 1980.
11. Singh, A.K. and Mazumdar, D., 1997. Mass transfer between solid and liquid in a gas-stirred vessel. Metallurgical and Materials Transactions B, 28(1), pp. 95-102.
12. Singh, R.P. and Ghosh, D.N., 1990. Cold Model Study of Liquid-Liquid Mass Transfer in a Combined Blowing BOS Converter. Ironmaking and Steelmaking, 17(5), pp. 333-342.
13. Szekely, J., Lehner, T. and Chang, C.W., 1979. Flow Phenomena, Mixing, and Mass Transfer in Argon-Stirred Ladles. Ironmaking Steelmaking, 6(6), pp. 285-293.
14. Vaarno, J., Pitkälä, J., Ahokainen, T. and Jokilaakso, A., 1998. Modelling gas injection of a Peirce-Smith-converter. Applied Mathematical Modelling, 22(11), pp. 907-920.
15. Versteeg, G.F., Blauwhoff, P.M.M. and Van Swaaij, W.P.M., 1987. The effect of diffusivity on gas-liquid mass transfer in stirred vessels - Experiments at atmospheric and elevated pressures. Chemical Engineering Science, 42(5), pp. 1103-1119.

Received August 28, 2011